Analytical and Bioanalytical Chemistry
https://doi.org/10.1007/s00216-018-1234-0

PAPER IN FOREFRONT

Analyte-driven self-assembly of graphene oxide sheets onto hydroxycamptothecin-functionalized upconversion nanoparticles for the determination of type I topoisomerases in cell extracts

Xu Wang[1] · Xiu-Ping Yan[2]

Received: 20 April 2018 / Revised: 28 May 2018 / Accepted: 28 June 2018

Abstract

Type I topoisomerases (TOPOI), a potential diagnostic biomarker and a target for chemotherapeutic agents, play essential roles in DNA replication, transcription, chromosome segregation, and recombination. It is essential to develop analytical methods for accurate detection of TOPOI in biological fluids for early diagnosis of diseases. Here we show an assay for TOPOI on the basis of the target-induced self-assembly of graphene oxide (GO) sheets onto hydroxycamptothecin-functionalized upconversion nanoparticles (HCPT-UCNPs). The dipole-dipole coupling of HCPT-UCNPs (donor) and GO (acceptor) regulated by TOPOI enables Förster resonance energy transfer between the donor and the acceptor. Integration of minimal autofluorescence and highly specific affinity into the developed nanosensor allows reliable detection of TOPOI in the nanomolar range with the detection limit of 0.29 nM. The detection of TOPOI in breast cancer cells with recoveries from 96.3 to 103.7% shows the availability of the proposed assay in complicated samples.

Keywords Type I topoisomerases · Hydroxycamptothecin · Upconversion nanoparticles · Graphene oxide · Biosensors

Introduction

Type I topoisomerases (TOPOI), belonging to the family of eukaryotic type IB topoisomerases, is a critical component of intracellular catalytic intermediate to regulate the topology of genomic DNA [1, 2]. The enzyme catalyzes the relaxation of supercoiled DNA by clamping on to the DNA helix, making a nick (cleavage reaction step), relaxing the stress by strand rotation, and rejoining the relaxed DNA by ligation (religation reaction step), followed by enzyme release. Besides its vital biological functions, TOPOI is recognized as a potential diagnostic biomarker as well as a target for chemotherapeutic agents due to an increased TOPOI activity in most cancer cells [3–5].

Camptothecin (CPT) family, a potent anticancer drug used in the systemic treatment of breast-, ovarian-, colon-, and small-cell lung cancer, solely targets TOPOI in a well-defined manner. CPTs act by selectively inhibiting the religation step of TOPOI catalysis by specifically binding the TOPOI-DNA cleavage intermediate. This leads to the accumulation of covalent cleavage intermediates in the genomic DNA, which further collide with the replication forks resulting in DNA fragmentation and ultimately cell death [6–8]. The cytotoxic effect of CPTs tightly correlates with the intracellular activity of TOPOI, thus enabling it possible to predict the CPTs' response in cancer cells via detection of TOPOI.

Current standard assays for TOPOI, such as DNA relaxation in combination with gel electrophoresis [9], Western blot

Published in the topical collection *New Insights into Analytical Science in China* with guest editors Lihua Zhang, Hua Cui, and Qiankun Zhuang.

Electronic supplementary material The online version of this article (https://doi.org/10.1007/s00216-018-1234-0) contains supplementary material, which is available to authorized users.

✉ Xiu-Ping Yan
xpyan@jiangnan.edu.cn; xpyan@nankai.edu.cn

[1] Tianjin Key Laboratory on Technologies Enabling Development of Clinical Therapeutics and Diagnostics (Theranostics), School of Pharmacy, Tianjin Medical University, Tianjin 300072, China

[2] State Key Laboratory of Food Science and Technology, Institute of Analytical Food Safety, School of Food Science and Technology, Jiangnan University, Wuxi 214122, China

Published online: 17 July 2018

analysis [10], enzyme-linked immunosorbent assays (ELISA) [11, 12], or immunohistochemical staining [13], are time-consuming and require specialized equipment and materials available only in fully equipped laboratories. Polymerase chain reaction (PCR) technique through detecting the level of mRNA instead of directly assaying TOPOI hardly indicates the dynamic enzymatic activity affected by post-translational modifications [14]. Recent developed DNA-based sensors offer attractive feature of fast detection of the cleavage-religation activity of TOPOI in real time through fluorescence resonance energy transfer (FRET) within a fluorophore–fluorophore pair or a fluorophore–quencher pair [15–17]. However, the accuracy in predicting the drug response of individual patients is still limited, as the other key influence on the efficiency of cancer treatment, namely the susceptibility of TOPOI towards drugs, is often ignored [18]. A sensitive and reliable assay for high-throughput measurement of TOPOI as well as direct reflection of the interaction of drug-TOPOI, thus, is of high clinical interest.

Herein, we report a new self-assembled FRET sensor for selective detection of TOPOI on the basis of hydroxycamptothecin (HCPT)-functionalized upconversion nanoparticles ($NaYF_4$:Yb, Gd, Er) (HCPT-UCNPs) and graphene oxide (GO) as the energy donor−acceptor pair. Upconversion nanoparticle (UCNP)-based nanosensors allow biodetection with minimal autofluorescence and reduced light scattering due to their unique optical properties, remarkably promoting the detection sensitivity in complicated biological samples in comparison to quantum dot-based or dye-based nanosensors [19–24]. HCPT as a recognition ligand is conjugated onto the surface of hyaluronic acid (HA)-grafted UCNPs (HA-UCNPs) to fabricate HCPT-UCNPs for capturing the target TOPOI in matrix. The overlap between the characteristic upconversion emission spectra of Er^{3+} ions at 540 and 660 nm in the donor HCPT-UCNPs and the UV–vis absorption spectra of the acceptor GO is a prerequisite for FRET. The FRET from HCPT-UCNPs to GO is inhibited in the absence of TOPOI and DNA due to electrostatic repulsion between the negatively charged HCPT-UCNPs and GO. However, the presence of TOPOI and DNA leads to TOPOI trapped in the complex with DNA, enabling TOPOI binding to HCPT-UCNPs to form a ternary complex. GO further assembles onto UCNPs due to the π–π interaction between TOPOI and GO, thus reducing the distance between HCPT-UCNPs and GO and allowing the FRET to occur. The quenching of upconversion luminescence (UCL) ascribed from the self-assembly of GO onto HCPT-UCNPs driven by TOPOI directly reflects the TOPOI activity and the sensitivity of TOPOI towards HCPT. A sensitive and selective nanosensor is developed for the detection of TOPOI. To our knowledge, no UCNP-based nanosensors exploiting CPTs as recognition ligands for the detection of TOPOI have been reported so far.

Material and methods

Materials and reagents

All reagents were of the highest available purity and of analytical grade at least. Ultrapure water (Hangzhou Wahaha Group Co. Ltd., Hangzhou, China) was used throughout this work. TOPOI was purchased from Takara Bio. Co. Ltd. (Dalian, China). A single-stranded DNA with the base sequence 5′-P-GCCCGTAAATCTAAGTCTTT TAGATCCTCTAGCTGCTAGAGGATCTAAAAGACTTA G-3′ and a nucleoprotein extraction kit were purchased from Sangon Biotech Co. Ltd. (Shanghai, China). HA (MW 8.9 KDa) was purchased from Freda Co. Ltd. (Shandong, China). 10-Hydroxycamptothecin (HCPT) was purchased from Chengdu Labooo Co. Ltd. (Chengdu, China). Natural graphite flakes with an average particle size of 20 μm were obtained from Qingdao Henlide Graphite Co. (Qingdao, China). $RE(NO_3)_3$ (RE: Y^{3+}, Yb^{3+}, Er^{3+}, Gd^{3+}) (99.99%), 4-dimethylaminopyridine (DMAP), *N*,*N*′-dicyclohexylcarbodiimide (DCC), ethylene glycol (EG), sodium dodecyl sulfate (SDS), sodium chloride (NaCl, 99.0%), and ammonium fluoride (NH_4F, 98+%) were obtained from Alfa Aesar Ltd. PBS solutions (0.2 M, pH 4.0–9.0) were used in the experiments.

Characterization

The morphology and microstructure of UCNPs and GO were characterized by JEM100CXII transmission electron microscopy (TEM). The X-ray diffraction (XRD) patterns were collected on a Rigaku D/max-2500 X-ray diffractometer (Rigaku, Tokyo, Japan) with Cu Kα radiation. Fourier transform infrared (FTIR) spectra (4000–400 cm^{-1}) were collected on a Magna-560 spectrometer (Nicolet, Madison, WI). Dynamic light scattering and zeta potential measurements were carried out on a Zeta-sizer Nano ZS spectrometer (Malvern Instruments, Worcestershire, UK). Absorption spectra were recorded on a UV-3600 UV–vis–NIR spectrophotometer (Shimadzu, Tokyo, Japan). Upconversion luminescence (UCL) spectra was measured on a PTI QM/TM/NIR fluorescence spectrometer (Birmingham, NJ, USA) fitted with an external 980-nm laser (Beijing Hi-Tech Optoelectronic Co., China) instead of internal excitation source.

Synthesis of HCPT-UCNPs

HA-UCNPs ($NaY_{0.48}F_4$:$Yb_{0.20}$, $Gd_{0.30}$, $Er_{0.02}$) was synthesized and characterized according to Wang et al. [25]. In a typical experiment for the synthesis of HCPT-UCNPs, HA-UCNPs (0.02 mmol) was dispersed in 10 mL of anhydrous CH_2Cl_2. Subsequently, DMAP (0.08 mmol) and HCPT (0.04 mmol) were added to form a homogeneous solution

under ultrasound in an ice bath. Then, 0.2 mmol of DCC in 10 mL of anhydrous CH_2Cl_2 was added dropwise into the solution, followed by stirring at 0 °C for 2 h and at room temperature for 24 h. The resulting HCPT-UCNPs were purified by centrifugation, washed with ethanol for three times, and dried in vacuum for 12 h.

Optimization of GO concentration

GO was synthesized from natural graphite flakes according to a modified Hummers' method [26]. Sonification of 1.0 mg mL^{-1} of GO aqueous solution was carried out in an ultrasonic bath (100 W, 50 °C) overnight for further experiments. After incubation with TOPOI (18 μL, 1.03 μM) and DNA (18 μL, 10.3 μM) for 30 min, the UCL of HCPT-UCNP solution (100 μL, 1.0 mg mL^{-1}) was determined with the increased concentrations of GO (0–300 μL, 1.0 mg mL^{-1}) in PBS (pH 5.0, 10 mM). The resulting mixture was diluted to 1.0 mL with PBS buffer (pH 5.0, 10 mM) before determination.

Procedures for TOPOI assay

In a typical assay, the mixture of HCPT-UCNPs (100 μL, 1.0 mg mL^{-1}) and GO (150 μL, 1.0 mg mL^{-1}) was incubated with different concentrations of TOPOI (0–40 μL, 1.03 μM) in PBS (pH 5.0, 10 mM) at 37 °C for 30 min. The concentration of DNA substrate (ca. 10 times excess compared to enzyme) is sufficient to keep a reaction with TOPOI at steady state. The resulting mixture was diluted to 1.0 mL with PBS buffer (pH 5.0, 10 mM) and was subjected to fluorescence measurement with the excitation of 980-nm laser.

The UCL quenching of HCPT-UCNPs by GO was monitored at 540 and 660 nm for detection of TOPOI. The energy transfer efficiency (I_d) was calculated as follows: $I_d = [I_0 - I]/[I_0] \times 100\%$, where I_0 is the UCL intensity of HCPT-UCNPs/GO in the absence of TOPOI and DNA, and I is the UCL intensity of HCPT-UCNPs/GO in the presence of TOPOI and DNA.

To examine the specificity of the developed HCPT-UCNPs/GO nanosensor for TOPOI detection, various biomolecules were added to the HCPT-UCNPs/GO aqueous solution in place of TOPOI with the same experimental conditions and procedures. The UCL spectra were recorded under the excitation of 980-nm laser.

Cell culture and preparation of nuclear extracts

MCF-7 and MDA-MB-231 cell lines were obtained from the China Center for Type Culture Collection (CCTCC) (Wuhan, China). MCF-7 and MDA-MB-231 cells were cultured in complete medium (Dulbecco's modified Eagle's medium, supplemented with 20% fetal bovine serum, 1% penicillin, and 1% streptomycin). Cells were harvested with 0.5% trypsin-EDTA and media was then discarded. Cells were subsequently washed with PBS buffer prior to nuclear extraction. Nuclear extraction was conducted using a nucleoprotein extraction kit following the manufacturer's directions. Briefly, 1×10^7 cells per milliliter were incubated in 1.0 mL of lysis buffer on ice for 10 min. After cell lysis, the nuclei were extracted in 200 μL of extraction buffer and used for subsequent tests.

Assay of TOPOI in cell nuclear extracts

Aliquots (2 μL) of the cell nuclear extract were added to the reaction mixture including HCPT-UCNPs (100 μL, 1.0 mg mL^{-1}), GO (150 μL, 1.0 mg mL^{-1}), and DNA (10 μL, 10.3 μM), followed by incubation at 37 °C for 30 min. The resulting solution was diluted to 1.0 mL with PBS buffer (pH 5.0, 10 mM), and then subjected to fluorescence measurement under the excitation of a 980-nm laser. The reaction mixture spiked with standard TOPOI (10 μL, 1.03 μM) was set as the control.

Estimation of TOPOI in cell nuclear extract by gel electrophoresis

SDS gel electrophoreses and coomassie brilliant staining were carried out as previously described [17]. Covalent attachment of active TOPOI to DNA resulted in a gel-electrophoretic retardation, allowing the fraction of active and inactive enzymes to be determined after staining with coomassie brilliant blue by quantification of the bands. The total amount of TOPOI in cell nuclear extract was calculated according to the intensity of the stained bands corresponding to the BSA or TOPOI with a known concentration.

Results and discussion

Design of an UCL assay for TOPOI

Scheme 1 illustrates the design and fabrication of the developed target-driven self-assembled nanosensor for the detection of TOPOI. The nanosensor employs HCPT-UCNPs and GO as the donor and the acceptor for FRET, respectively. To achieve highly specific and sensitive detection of TOPOI in complex matrix, HCPT, usually applied in chemotherapeutic treatment of various cancers, was exploited as a recognition ligand.

HCPT kills cancerous cells through inhibiting the religation step of TOPOI catalysis (see Electronic Supplementary Material (ESM), Scheme S1). The catalytic cycle of TOPOI is triggered by the active site tyrosine (Tyr723) through a nucleophilic attack on the DNA backbone, resulting in the

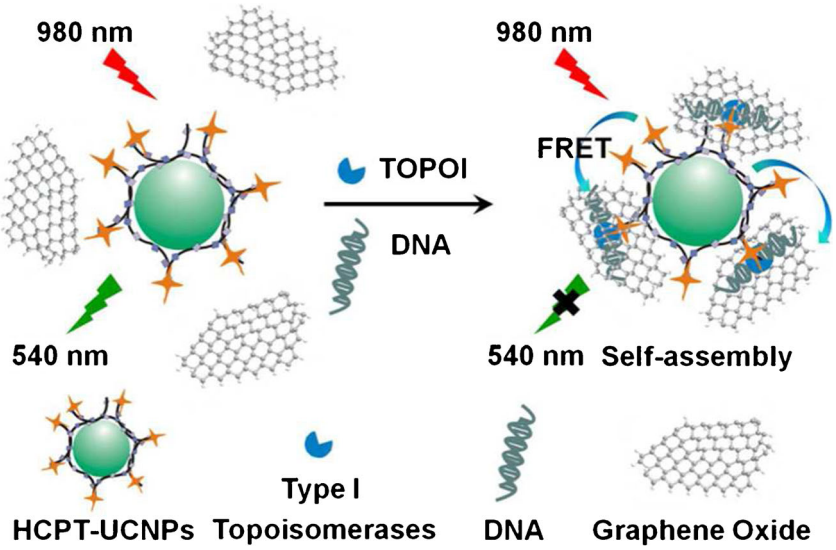

Scheme 1 Illustration for the design and principle of TOPOI-driven assembled nanosensor for TOPOI detection

breakage of one DNA strand. This facilitates the enzyme covalently attached onto DNA to form the cleavage TOPOI-DNA complex. In general, the cleavage complex is transient, followed by a religation step leading to a nick-closing reaction of DNA. Meanwhile, the enzyme is released from the backbone of DNA. However, in the presence of HCPT, it intercalates into the base pairs that flank the cleavage site (nick), inhibiting the ends of the cleaved DNA strand aligned for efficient religation. A newly formed ternary complex further converts a single-DNA-strand break into double-DNA-strand breaks upon collision with the replication machinery, which finally results in cell death [8, 27]. As the sole cellular target of HCPT, TOPOI can be selectively captured by HCPT-UCNPs for further detection.

To simulate the role of HCPT (ESM, Scheme S1), an appropriate design of DNA as substrates for TOPOI catalysis was made. A phosphate group at the 5′-end for providing a short nucleotide sequence downstream the cleavage site (GACTT*AG) was set to control the progress of reaction after cleavage. In such a situation, the enzyme is able to cleave the DNA to form the TOPOI-DNA binary complex, but the religation step is prevented because the generated dinucleotide downstream of the binding site diffuses away from the complex [28].

In the absence of TOPOI and DNA, the FRET is hard to occur due to electrostatic repulsion of the negatively charged HCPT-UCNPs and GO. No obvious change in the UCL of HCPT-UCNPs can be observed. After adding TOPOI and DNA, TOPOI is involved in a complex with DNA and thereby binds to HCPT-UCNPs to form a ternary complex (TOPOI/DNA/HCPT-UCNPs). GO further assembles onto UCNPs due to the π–π interaction between TOPOI and GO, thus reducing the distance between HCPT-UCNPs and GO and allowing the FRET to occur. The UCL quenching as a result of GO assembled onto UCNPs induced by TOPOI provides a sensing platform for the detection of TOPOI with high specificity and sensitivity.

Synthesis and characterization of HCPT-UCNPs and GO

The HCPT-UCNPs as the energy donor was constructed from HA-UCNPs and HCPT via the esterification condensation. The HA-UCNPs involved in the donor gave strong multicolor upconversion luminescence at 540 and 660 nm (Fig. 1a), overlapping with the high UV–vis absorption spectra of the acceptor GO. HA was used as a functional ligand for further conjugation with HCPT due to its rich active chemical groups with repeated D-glucuronic acid and *N*-acetyl-D-glucosamine units. After conjugation of HCPT onto the surface of HA-UCNPs, the formed HCPT-UCNPs were capable of selective capturing of the target from the complicated matrix based on the high affinity of HCPT towards TOPOI.

To obtain optimal loading of HCPT, a feeding HCPT:HA-UCNP molar ratio of 2:1 was used for the preparation of HCPT-UCNPs (ESM, Fig. S1). The as-prepared HCPT-UCNPs show strong distinct luminescence peaks at 455 and 575 nm of HCPT under UV irradiation (365 nm), indicating the successful conjugation of HCPT onto UCNPs (Fig. 1a; ESM, Fig. S1). The fluorescence intensity of HCPT-UCNPs at 455 nm reveals 5.1 HCPT molecules modified onto each HCPT-UCNP on average.

The size and morphology of the synthesized HCPT-UCNPs were characterized by TEM. The prepared HCPT-UCNPs are spherical with an average size of 25.0 ± 3.2 nm (ESM, Fig. S2a). The covalent binding of HCPT to HA-UCNPs was further verified with zeta potential, UV–vis spectroscopy, and FTIR. Upon attachment of HCPT to HA-UCNPs, the zeta potential became more negative (− 31.7 mV) in PBS (pH 5.0, 10 mM) (Fig. 1b). The

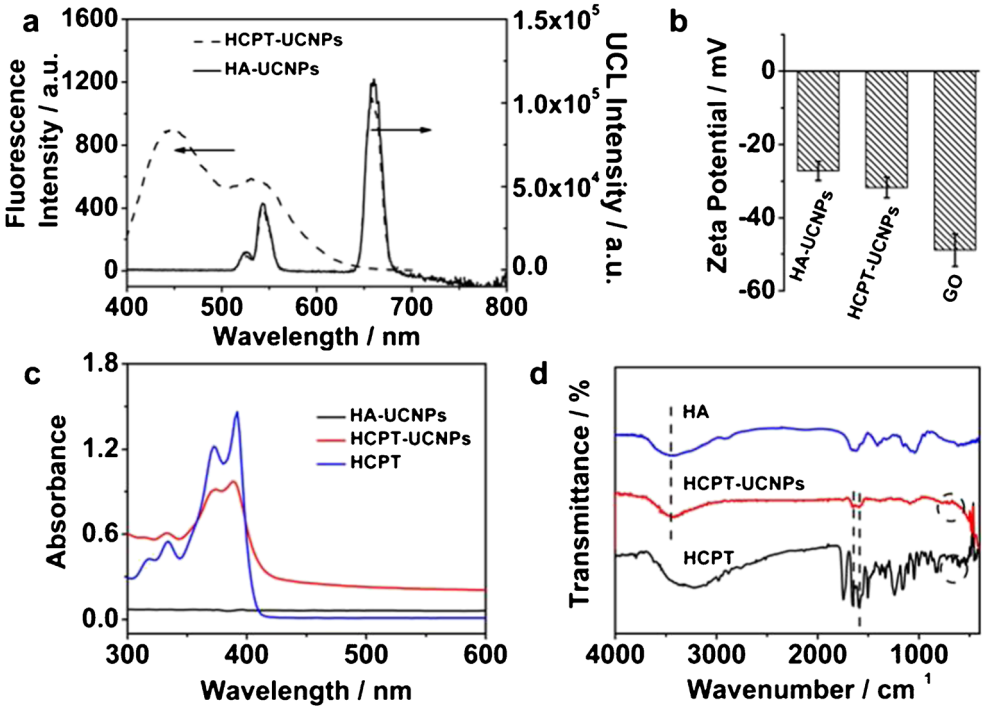

Fig. 1 Characterization of HCPT-UCNPs and GO. **a** Fluorescence spectra of HCPT-UCNPs (365 nm excitation, dashed line) and upconversion luminescence spectra of HA-UCNPs (0.02 wt%, black solid line) and HCPT-UCNPs (0.02 wt%, dashed line) aqueous solution (980 nm excitation). **b** Zeta potential of HA-UCNPs, HCPT-UCNPs, and GO in PBS (pH 5.0, 10 mM). **c** Comparison of UV–vis absorption spectra of HA-UCNPs, HCPT-UCNPs, and HCPT in PBS (pH 5.0, 10 mM). **d** FTIR spectra of HA-UCNPs, HCPT-UCNPs, and HCPT

presence of the characteristic absorption band (around 380 nm) of HCPT in the UV–vis spectra of HCPT-UCNPs also shows the successful immobilization of HCPT on the surface of UCNPs (Fig. 1c). FTIR spectra provide further evidence for HCPT attachment. The characteristic peaks at 1650.9 and 1589.1 cm^{-1} for the absorption bands of carbonyl group in ester bond and N–H bond in the FTIR spectrum of HCPT-UCNPs confirm the successful conjugation of HCPT to HA-UCNPs (Fig. 1d) [29]. HCPT-UCNPs possess good colloidal stability as no any visible precipitation was observed after incubation in PBS (pH 5.0, 10 mM) for at least 2 weeks. Also, no obvious change in the UCL of HCPT-UCNPs was observed by continuous irradiation with 980-nm laser for 60 min, revealing the good photostability of HCPT-UCNPs.

GO with high solubility and stability facilitates noncovalent interaction with proteins through π–π stacking and hydrogen bonding, which is thus recognized as an ideal choice as an energy transfer acceptor. The synthesized GO typically presents a high planar surface, enabling an increased number of UCNPs adsorbed onto the surface of GO (ESM, Fig. S2b) [30]. The XRD pattern of the as-prepared GO exhibits the characteristic diffraction peak of GO at $2\theta = 11.86°$ (ESM, Fig. S3) [31]. A red brown of GO water colloid displays typical optical properties of chemically prepared GO, with two characteristic absorption peaks at 230 and 300 nm originating from π–π* transition of the C=C band and *n*–π* transition of the C=O band, respectively (ESM, Fig. S4) [32]. The wide absorbance from 200 to 700 nm overlapped with the emission of the donor HCPT-UCNPs allows FRET to occur. The zeta potential (− 48.9 mV) of the colloidal GO in PBS (pH 5.0, 10 mM) indicates the excellent dispersibility of GO in aqueous solution (Fig. 1b).

Construction of the HCPT-UCNPs/GO nanosensor

As shown in Fig. 2, background signal of the assay was determined by incubating HCPT-UCNPs (100 μg mL^{-1}) with GO (150 μg mL^{-1}), demonstrating a slight decrease of the UCL of HCPT-UCNPs (~ 23%). The weak UCL quenching of HCPT-UCNPs was ascribed to the UCL being partly shielded by the black GO solution [33]. Addition of DNA into the mixture of HCPT-UCNPs and GO led to no obvious change in UCL, indicating DNA itself had little impact on the FRET between donor and acceptor. In contrast, maximum quenching occurred upon the addition of both TOPOI and DNA, which took the energy donor and the acceptor in close proximity to promote the FRET process. It should be noted that the HCPT-UCNPs/GO nanosensor also made response to TOPOI even without DNA in the matrix, probably due to the non-specific absorption of TOPOI onto the donor–acceptor pair [34]. However, in this case, a complete quenching of the donor can hardly be achieved as a stable complex stabilized by HCPT-UCNPs cannot be formed in the absence of DNA.

To further demonstrate the target-induced UCL quenching on the basis of GO attached onto UCNPs, a control experiment was conducted by incubating HA-UCNPs (100 μg mL^{-1}) in place of HCPT-UCNPs with GO (150 μg mL^{-1}) in the presence

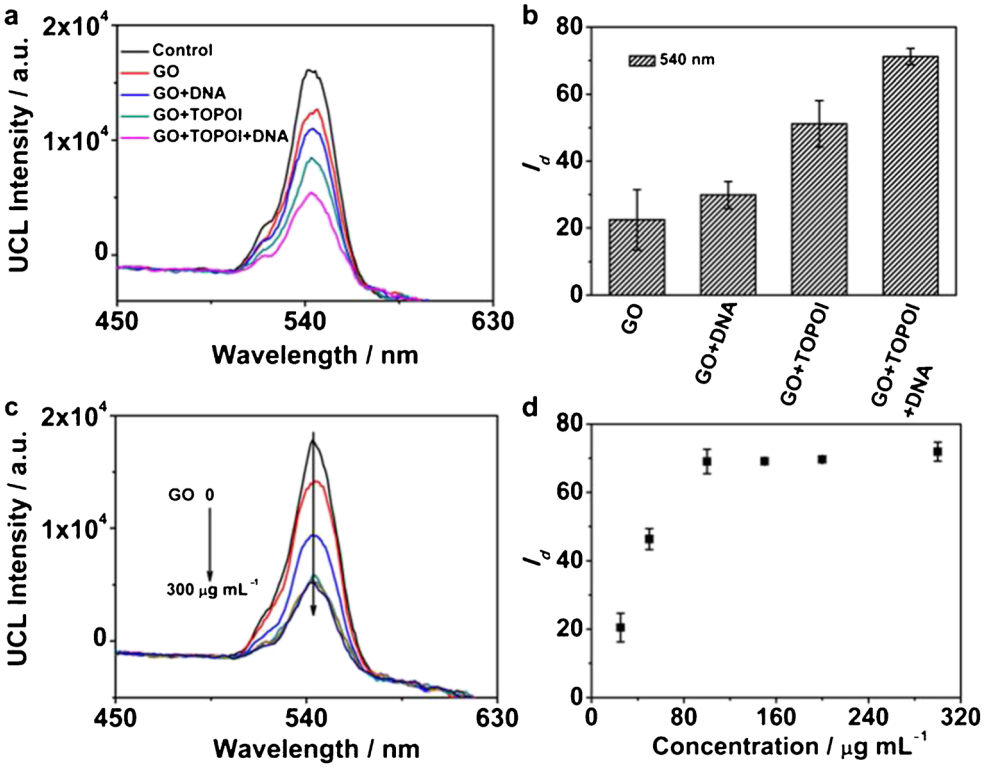

Fig. 2 Construction of the HCPT-UCNPs/GO nanosensor. **a**, **b** Comparison of HCPT-UCNPs (100 μg mL^{-1}) before and after incubation with GO (150 μg mL^{-1}), HCPT-UCNPs after incubation with GO upon the addition of only DNA (186 nM), only TOPOI (18.6 nM), or both TOPOI (18.6 nM) and DNA (186 nM), respectively: **a** UCL spectra centered at 540 nm. **b** The energy transfer efficiency (I_d) of HCPT-UCNPs and GO. **c** UCL spectra of HCPT-UCNPs (100 μg mL^{-1}) after incubation with different concentrations of GO (0–300 μg mL^{-1}) in the presence of TOPOI (18.6 nM) and DNA (186 nM). **d** The corresponding plot of the energy transfer efficiency (I_d) of HCPT-UCNPs recorded at 540 nm versus GO concentration

of TOPOI and DNA. As expected, the UCL of HA-UCNPs remained nearly unchanged (ESM, Fig. S5), suggesting the key role of HCPT in the interaction with the TOPOI-DNA cleavage intermediate.

Optimization of the HCPT-UCNPs/GO nanosensor

For ensuring the high efficiency of FERT, the optimal concentration of GO was investigated. Figure 2c shows that the UCL

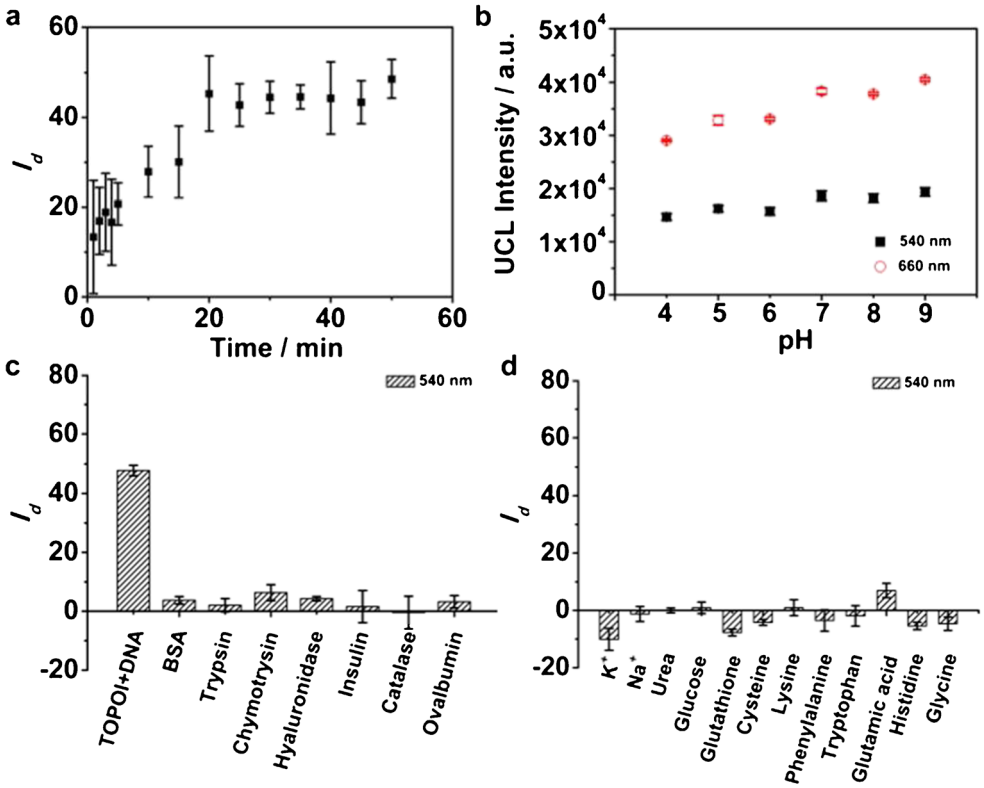

Fig. 3 Optimization of the HCPT-UCNPs/GO nanosensor and specificity. **a** The energy transfer efficiency (I_d) of HCPT-UCNPs (100 μg mL^{-1}), GO (150 μg mL^{-1}), and DNA (186 nM) in presence of TOPOI (18.6 nM) as a function of time. **b** Effect of pH on the UCL intensity of HCPT-UCNPs/GO for the detection of TOPOI (18.6 nM). **c**, **d** Specificity test of the developed HCPT-UCNPs/GO nanosensor for the detection of TOPOI (18.6 nM) over other biomolecules and inorganic ions. Concentrations: amino acids, 100 μM; K^+ and Na^+, 10 mM; BSA (10 μM), trypsin (100 U mL^{-1}), chymotrypsin (100 U mL^{-1}), hyaluronidase (100 U mL^{-1}), insulin (10 μM), catalase (100 U mL^{-1}), and ovalbumin (10 μM)

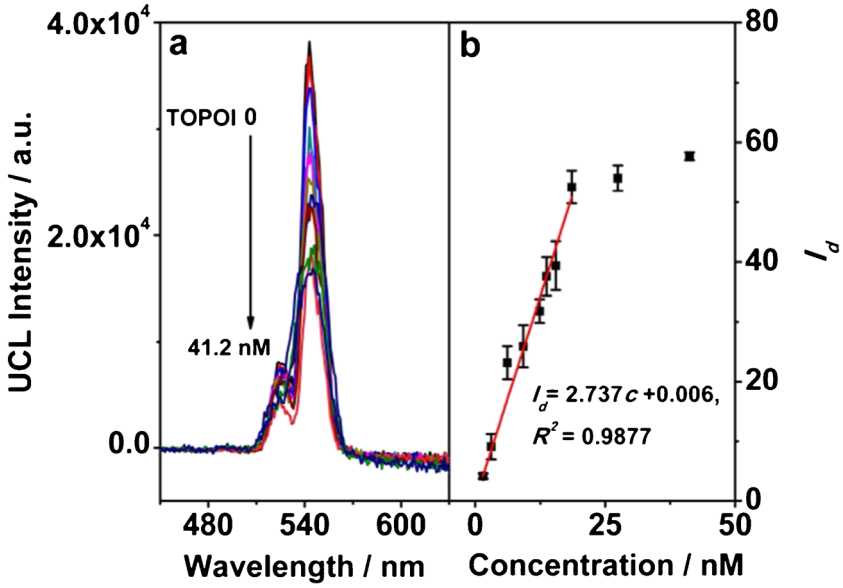

Fig. 4 Analytical performance of the TOPOI-driven self-assembled nanosensor. (**a**) Change of the UCL spectra of the HCPT-UCNPs/GO nanosensor with the concentration of TOPOI. (**b**) Energy transfer efficiency as a function of the concentration of TOPOI. All solutions were prepared in PBS (10 mM, pH 5.0)

decreased proportionally as the concentration of GO increased from 25 to 100 μg mL^{-1}, then leveled off with a further increase of the concentration of GO. The optimum concentration of GO was selected as 150 μg mL^{-1}, giving nearly 70% UCL quenching (Fig. 2d). The excellent quenching capability and water solubility make GO a good quencher to fabricate the UCNP-based nanosensor.

To monitor the UCL quenching of HCPT-UCNPs/GO induced by TOPOI, time-dependent UCL quenching experiments were conducted by adding TOPOI (18.6 nM) into the mixture of HCPT-UCNPs (100 μg mL^{-1}), GO (150 μg mL^{-1}), and DNA (186 nM). Figure 3a shows that the maximum FRET efficiency reached after 20 min, and a platform was observed for a further 30 min. An adequate quenching cannot be achieved until the TOPOI-DNA binary complex is completely formed, which promotes the FRET between HCPT-UCNPs and GO. An excess concentration of DNA substrate (ca. 10 times excess compared to enzyme) is set to keep a sufficient reaction with TOPOI at steady state.

The effect of pH on the UCL of HCPT-UCNPs/GO in the presence of TOPOI and DNA was also optimized over the range of 4.0–9.0. Figure 3b shows that the quenching efficiency decreased with the increase of pH due to the reduced stability of the ester bond in HCPT-UCNPs at higher pH value (> 7.0). To show the effect of pH on the stability of HCPT-UCNPs, a batch of assay was designed by detecting the fluorescence of released HCPT in supernate from HCPT-UCNP solution in the pH range of 4.4–8.0 (ESM, Fig. S6). The fluorescence intensity at 575 nm increased with pH, indicating the enhanced release of HCPT from the surface of UCNPs at higher pH value. Relatively high pH (> 7.0) results in the cleavage of the ester bond between HCPT and UCNPs, hindering the binding of HCPT-UCNPs towards the TOPOI-DNA complex. To obtain better sensitivity, pH 5.0 was selected as the optimum pH condition.

Specificity of the HCPT-UCNPs/GO nanosensor

To test the specificity of the developed HCPT-UCNPs/GO nanosensor for TOPOI detection, common biomolecules of proteins and enzymes, inorganic ions, and amino acids in tumor cells were chosen to test their response to the sensor under the same conditions for TOPOI determination (Fig. 3c, d). The tested inorganic ions or amino acids (100 μM), serum proteins, and enzymes such as BSA (10 μM), trypsin

Table 1 Analytical results for TOPOI in human cell extracts

Sample	Spiked (nM)	Concentration of TOPOI (nM) (mean ± s, $n = 3$)		Recovery (%) (mean ± s, $n = 3$)
		SDS gel electrophoreses	This method	
MCF-7 cell	0	1.98 ± 0.12	2.07 ± 0.47	–
	10.30	–	12.69 ± 0.42	103.7 ± 4.1
MDA-MB-231 cell	0	Not detectable	Not detectable	–
	10.30	–	9.92 ± 0.75	96.3 ± 7.3

(100 U mL^{-1}), chymotrypsin (100 U mL^{-1}), hyaluronidase (100 U mL^{-1}), insulin (10 μM), catalase (100 U mL^{-1}), and ovalbumin (10 μM) produced negligible response to the developed HCPT-UCNPs/GO biosensor. All the above data indicate the excellent selectivity of our proposed HCPT-UCNPs/GO nanosensor towards TOPOI.

Analytical performance of the HCPT-UCNPs/GO nanosensor

Under the optimal conditions, calibration of the sensor was achieved by adding various concentrations of TOPOI ranging from 1.5 to 41.2 nM to a fixed concentration of HCPT-UCNPs/GO (100/150 μg mL^{-1}) nanosensor (Fig. 4). The luminescence quenching efficiency increased with the concentration of TOPOI in the range of 1.5 to 18.6 nM, then leveled off with a further increase of the concentration of TOPOI. A linear calibration plot of the luminescence quenching efficiency against the concentration of TOPOI from 1.5 to 18.6 nM was obtained with the linear regression equation of $I_d = 0.274\ C + 0.006$ ($R^2 = 0.9877$). The proposed method gave a detection limit (3 s) of 0.29 nM for the detection of TOPOI. The precision for 11 replicate determinations of TOPOI at 9.3 nM is 2.8% RSD. The proposed method exhibits comparable or lower detection limit compared with most of the methods for the detection of TOPOI (ESM, Table S1). Though the proposed method has higher detection limit than the rolling circle amplification-based assay, it owns the merit of faster detection without the use of complex instrumentation (ESM, Table S1).

Application to cell extracts

To demonstrate its applicability in real sample analysis, the developed HCPT-UCNPs/GO nanosensor was applied for specific detection of TOPOI in cell extracts. The nanosensor was tested using the standard TOPOI spiked-in human nuclear extract from MCF-7 and MDA-MB-231 cells (Table 1). The recoveries of the spiked analytes in the samples ranged from 96.3 to 103.7%, demonstrating the potential applicability for TOPOI detection in biological samples. The detection was minimally affected in the presence of human cell extracts, containing human topoisomerases along with other eukaryotic proteins. To further verify the reliability of the nanosensor, the standard method of SDS gel electrophoresis was applied for detecting TOPOI in human nuclear extract from MCF-7 and MDA-MB-231 cells. The concentrations of TOPOI in cell extracts obtained by the proposed method are in good agreement with those obtained by SDS gel electrophoresis (Table 1; ESM, Fig. S7). The advantages of the proposed approach presented is relatively fast and easy to perform and requires only very little enzyme compared to standard method.

Conclusions

In conclusion, we have developed a simple and smart luminescence assay based on HCPT-UCNPs/GO nanosensor for detection of TOPOI with high sensitivity and specificity. The coupling of donor–acceptor pair specifically mediated by TOPOI promotes the efficiency of FRET, resulting in the luminescence quenching of the energy donor. It is possible to follow the enzyme substrate interactions at nanomolar enzyme concentrations thereby directly detecting the TOPOI activity and reflecting the HCPT susceptibility in clinical relevant patient samples. Using such a strategy, it is straightforward to exploit the sensor for a realistic application where the amount of enzyme present in a crude sample is unknown.

Funding information This study received financial support from the National Natural Science Foundation of China (Nos. 21435001 and 81401471), the China Postdoctoral Science Foundation (No. 2015 M581306), the Natural Science Foundation of Tianjin (No. 17JCYBJC20700), the Natural Science Foundation of Tianjin Medical University (No. 2014KYQ14), and the National First-class Discipline Program of Food Science and Technology (No. JUFSTR20180301).

Compliance with ethical standards

Conflict of interest The authors declare that they have no conflict of interest.

References

1. Champoux JJ. DNA topoisomerases: structure, function, and mechanism. Annu Rev Biochem. 2001;70:369–413.
2. Wang JC. Cellular roles of DNA topoisomerases: a molecular perspective. Nat Rev Mol Cell Biol. 2002;3(6):430–40.
3. Giovanella BC, Stehlin JS, Wall ME, Wani MC, Nicholas AW, Liu LF, et al. DNA topoisomerase I—targeted chemotherapy of human colon cancer in xenografts. Science. 1989;246(4933):1046–8.
4. Hsiang YH, Liu LF. Identification of mammalian DNA topoisomerase I as an intracellular target of the anticancer drug camptothecin. Cancer Res. 1988;48(7):1722–6.
5. Pommier Y. Topoisomerase I inhibitors: camptothecins and beyond. Nat Rev Cancer. 2006;6(10):789–802.
6. Basili S, Moro S. Novel camptothecin derivatives as topoisomerase I inhibitors. Expert Opin Ther Pat. 2009;19(5):555–74.
7. Slichenmyer WJ, Rowinsky EK, Donehower RC, Kaufmann SH. The current status of camptothecin analogues as antitumor agents. J Natl Cancer Inst. 1993;85(4):271–91.
8. Sriram D, Yogeeswari P, Thirumurugan R, Bal TR. Camptothecin and its analogues: a review on their chemotherapeutic potential. Nat Prod Res. 2005;19(4):393–412.
9. Webb MR, Ebeler SE. A gel electrophoresis assay for the simultaneous determination of topoisomerase I inhibition and DNA intercalation. Anal Biochem. 2003;321(1):22–30.
10. Liebes L, Potmesil M, Kim T, Pease D, Buckley M, Fry D, et al. Pharmacodynamics of topoisomerase I inhibition: western blot determination of topoisomerase I and cleavable complex in patients with upper gastrointestinal malignancies treated with topotecan. Clin Cancer Res. 1998;4(3):545–57.

11. Pfister TD, Reinhold WC, Agama K, Gupta S, Khin SA, Kinders RJ, et al. Topoisomerase I levels in the NCI-60 cancer cell line panel determined by validated ELISA and microarray analysis and correlation with indenoisoquinoline sensitivity. Mol Cancer Ther. 2009;8(7):1878–84.
12. Sato S, Hamaguchi Y, Hasegawa M, Takehara K. Clinical significance of anti-topoisomerase I antibody levels determined by ELISA in systemic sclerosis. Rheumatology. 2001;40(10):1135–40.
13. Hafian H, Venteo L, Sukhanova A, Nabiev I, Bt L, Pluot M. Immunohistochemical study of DNA topoisomerase I, DNA topoisomerase IIα, p53, and Ki-67 in oral preneoplastic lesions and oral squamous cell carcinomas. Hum Pathol. 2004;35(6):745–51.
14. Skrzypski M. Quantitative reverse transcriptase real-time polymerase chain reaction (qRT-PCR) in translational oncology: lung cancer perspective. Lung Cancer. 2008;59(2):147–54.
15. Jepsen ML, Harmsen C, Godbole AA, Nagaraja V, Knudsen BR, Ho Y-P. Specific detection of the cleavage activity of mycobacterial enzymes using a quantum dot based DNA nanosensor. Nanoscale. 2016;8(1):358–64.
16. Jepsen ML, Ottaviani A, Knudsen BR, Ho Y-P. Quantum dot based DNA nanosensors for amplification-free detection of human topoisomerase I. RSC Adv. 2014;4(5):2491–4.
17. Kristoffersen EL, Jorgensen LA, Franch O, Etzerodt M, Frohlich R, Bjergbaek L, et al. Real-time investigation of human topoisomerase I reaction kinetics using an optical sensor: a fast method for drug screening and determination of active enzyme concentrations. Nanoscale. 2015;7(21):9825–34.
18. Marcussen LB, Jepsen ML, Kristoffersen EL, Franch O, Proszek J, Ho Y-P, et al. DNA-based sensor for real-time measurement of the enzymatic activity of human topoisomerase I. Sensors. 2013;13(4):4017–28.
19. Gorris HH, Resch-Genger U. Perspectives and challenges of photon-upconversion nanoparticles—part II: bioanalytical applications. Anal Bioanal Chem. 2017;409(25):5875–90.
20. Liu J, Liu Y, Liu Q, Li C, Sun L, Li F. Iridium(III) complex-coated nanosystem for ratiometric upconversion luminescence bioimaging of cyanide anions. J Am Chem Soc. 2011;133(39):15276–9.
21. Guo X, Wu S, Duan N, Wang Z. Mn^{2+}-doped $NaYF_4$:Yb/Er upconversion nanoparticle-based electrochemiluminescent aptasensor for bisphenol A. Anal Bioanal Chem. 2016;408(14):3823–31.
22. Hua X, You H, Luo P, Tao Z, Chen H, Liu F, et al. Upconversion fluorescence immunoassay for imidaclothiz by magnetic nanoparticle separation. Anal Bioanal Chem. 2017;409(29):6885–92.
23. Peng J, Xu W, Teoh CL, Han S, Kim B, Samanta A, et al. High-efficiency in vitro and in vivo detection of Zn^{2+} by dye-assembled upconversion nanoparticles. J Am Chem Soc. 2015;137(6):2336–42.
24. Wu S, Duan N, Zhang H, Wang Z. Simultaneous detection of microcysin-LR and okadaic acid using a dual fluorescence resonance energy transfer aptasensor. Anal Bioanal Chem. 2015;407(5):1303–12.
25. Wang X, Chen J-T, Zhu H, Chen X, Yan X-P. One-step solvothermal synthesis of targetable optomagnetic upconversion nanoparticles for in vivo bimodal imaging. Anal Chem. 2013;85(21):10225–31.
26. Hummers WS, Richard EO. Preparation of graphitic oxide. J Am Chem Soc. 1958;80:1339.
27. Beretta GL, Perego P, Zunino F. Targeting topoisomerase I: molecular mechanisms and cellular determinants of response to topoisomerase I inhibitors. Expert Opin Ther Targets. 2008;12(10):1243–56.
28. Zuccaro L, Tesauro C, Kurkina T, Fiorani P, Yu HK, Knudsen BR, et al. Real-time label-free direct electronic monitoring of topoisomerase enzyme binding kinetics on graphene. ACS Nano. 2015;9(11):11166–76.
29. Li G, Li Y, Tang Y, Zhang Y, Zhang Y, Yin T, et al. Hydroxyethyl starch conjugates for improving the stability, pharmacokinetic behavior and antitumor activity of 10-hydroxy camptothecin. Int J Pharm. 2014;471(1–2):234–44.
30. Loh KP, Bao Q, Eda G, Chhowalla M. Graphene oxide as a chemically tunable platform for optical applications. Nat Chem. 2010;2(12):1015–24.
31. Wang Y, Chen J-T, Yan XP. Fabrication of transferrin functionalized gold nanoclusters/graphene oxide nanocomposite for turn-on near-infrared fluorescent bioimaging of cancer cells and small animals. Anal Chem. 2013;85:2529–35.
32. Chen J-L, Yan X-P, Meng K, Wang S-F. Graphene oxide based photoinduced charge transfer label-free near-infrared fluorescent biosensor for dopamine. Anal Chem. 2011;83(22):8787–93.
33. Wu S, Duan N, Ma X, Xia Y, Wang H, Wang Z, et al. Multiplexed fluorescence resonance energy transfer aptasensor between upconversion nanoparticles and graphene oxide for the simultaneous determination of mycotoxins. Anal Chem. 2012;84(14):6263–70.
34. Siu F-M, Che C-M. Persistence of camptothecin analog-topoisomerase I-DNA ternary complexes: a molecular dynamics study. J Am Chem Soc. 2008;130(52):17928–37.

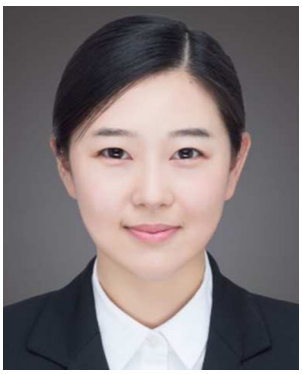

Xu Wang is in the School of Pharmacy, Tianjin Medical University, Tianjin, China. Her research interest focuses on nanomedicine, particularly on the development of functional nanomaterials for novel cancer theranostics, as well as the behaviors of nanomaterials in biological systems and nanotoxicology.

Xiu-Ping Yan is a Cheung Kong Distinguished Professor in the School of Food Science and Technology, Jiangnan University, Wuxi, China. His research focuses on hyphenated techniques and advanced materials for analytical chemistry, biomedical science, and food safety.